9-1994

# Effects Of Aberrations On Spatially Modulated Fourier Transform Spectrometers

R Glenn Sellar

James Bruce Rafert

# Effects of aberrations on spatially modulated Fourier transform spectrometers

**R. Glenn Sellar**
**J. Bruce Rafert,** MEMBER SPIE
Florida Institute of Technology
Department of Physics and Space Sciences
150 West University Boulevard
Melbourne, Florida 32901
E-mail: 105278@roo.fit.edu

**Abstract.** Spatially modulated Fourier transform spectrometers (FTS) have a throughput advantage over dispersive spectrometers, since an FTS does not require a slit in order to achieve spectral resolution. The traditional implementation of FTSs employs a scanning Michelson interferometer, but since this interferometer is temporally modulated, it is difficult or impossible to use with a target whose spatial and/or spectral signature is changing rapidly. The less common *spatially* modulated approach to FTS allows all spectral channels to be acquired simultaneously, but cylindrical optics are required to create an imaging version of this type of spectrometer [an imaging fourier transform spectrometer (IFTS)]. This combination of cylindrical and spherical optics, used to achieve both spectral and spatial resolution, increases the difficulty of understanding and controlling the aberrations. An understanding of the effects of these aberrations is essential to developing a spatially modulated IFTS with good spectral and spatial resolution. A spatially modulated IFTS based on a Sagnac interferometer is described, and the effects of aberrations on the spectral resolution, spatial resolution, and modulation are discussed.

*Subject terms: Fourier transform spectrometer; Sagnac interferometer; triangle-path interferometer; stationary interferometer; interferometry; aberrations.*

*Optical Engineering 33(9), 3087–3092 (September 1994).*

## 1 Introduction

The throughput advantages of Fourier transform spectrometers (FTS) are well known, but the drawbacks of the traditional, temporally modulated instruments have encouraged the development of spatially modulated implementations of FTSs.[1–5] The spatially modulated approach has the advantage of having no moving parts, avoiding the expense and vibration sensitivity of the mirror scanning system, and it allows simultaneous acquisition of all spectral information. These spatially modulated systems are particularly attractive for applications where the target and/or the instrument is moving, or where the spectral characteristics of the target are changing rapidly. The disadvantages of this approach are that spatial information is obtained in only one dimension, and that a combination of spherical and cylindrical optics is utilized. The second spatial dimension can be recovered by use of a field-scanning mirror or slit, or by moving the platform itself; but the difficulties with aberrations remain.

In the IR, where FTS is most often applied, these aberrations are relatively small in terms of waves, and the available array detectors are of low resolution; so there has not, in the past, been much of a requirement to minimize them. This requirement has, however, been growing in importance for two reasons: the steady increase in the number of elements in IR arrays, and the interest in applying this type of FTS at visible wavelengths. Thus, an understanding of the effect of aberrations on the performance of these instruments is essential in order to extend their range of applications.

Different designs for spatially modulated IFTSs have been built by a number of investigators.[1–5] One such instrument, for use at visible wavelengths, was built by Rafert et al.[5] This instrument is based on a triangle-path Sagnac interferometer as shown in Fig. 1. This particular instrument has been used for observations of satellites and launch-vehicle plumes (for the U.S. Air Force Phillips Laboratory), but could also be employed for other applications, such as remote sensing and astronomy. It is divided into five major subsystems: the fore-optics (a telescope in this case), the interferometer itself, a Fourier optic, a cylindrical imaging optic, and the detector. The telescope is used to form a 2-D spatial image at the input to the interferometer. This plane is the image plane for the telescope and the object plane for the Fourier optic. In these instruments, this plane was conveniently placed just in front of the beamsplitter, but it could be positioned deeper within the interferometer in order to improve the focal ratio that the interferometer can accept.

The interferometer itself is a Sagnac, or triangle-common-path, interferometer as shown in Fig. 2. When the interferometer mirrors are placed at identical distances from the beamsplitter, the reflected and transmitted rays will follow exactly the same path but in opposite directions. If one of the mirrors is offset from this position, however, then the rays emerge offset to either side of the central axis. The effect of this is to produce a pair of virtual objects that are mutually

Paper 09113 received Nov. 6, 1993; revised manuscript received Mar. 1, 1994; accepted for publication Mar. 2, 1994.

coherent and thus produce an interference pattern. The Fourier optic is placed one focal length from the object plane, and the detector is placed one focal length behind the Fourier optic (Fig. 1). Thus, the interference pattern imaged on the detector is the pattern that would be observed at an *infinite* distance from the objects if there were no Fourier optic. This removes any dependence of the interference pattern on the shape of the aperture. The interference pattern of a monochromatic source will be a pattern of vertical fringes whose spatial frequency $\nu$ is given by

$$\nu = \frac{s}{f\lambda} , \tag{1}$$

where $s$ is the separation between the virtual objects, $f$ is the focal length of the Fourier optic, $\lambda$ is the wavelength; we have assumed that $s$ is much smaller than $f$. A broadband source will produce a superposition of fringe patterns with many spatial frequencies. The one-dimensional Fourier transform of this interference pattern gives the spectrum of the source.

With the Fourier optic alone, we would have no *spatial* resolution at all, since rays from a point in the object plane will be collimated by the Fourier optic. The interference pattern, however, is only modulated in the plane of the interferometer (for this example the horizontal plane), so the other dimension (the vertical) is redundant. Since this redundant dimension carries no spectral information, it can be used for spatial information. When a cylindrical optic is placed one focal length from the detector and oriented so that it has power only in the vertical direction (Fig. 1), the object is imaged onto the detector in the vertical direction. Thus we acquire spatial resolution in this one dimension.

Note that, unlike a dispersive instrument, no slit is required in the object plane. This provides a great advantage in throughput over dispersive instruments. A slit is only required if we need to recover the second spatial dimension (the horizontal) by scanning a slit across the object plane, or by using a mirror to scan the object across the slit. In this case there is a tradeoff between throughput and horizontal spatial resolution, but the *spectral* resolution remains independent of the slit width. Thus we can optimize the throughput versus horizontal spatial resolution and the throughput versus spectral resolution *independently*, unlike the case of a dispersive instrument, where both the spectral resolution and the horizontal spatial resolution are tied to the slit width.

Before entering into a discussion on the effects of aberrations in this type of instrument, it must be pointed out that the Seidel, Zernike, and wavefront coefficients,[6] while often used to categorize the aberrations of a system, are not appropriate for this instrument. These coefficients are all defined in polar coordinates, and thus assume a rotationally symmetric optical system. Although terms such as ''distortion'' are used in this paper, we use them in their more general sense, not as a reference to a Seidel, Zernike, or wavefront coefficient. The development of a system of aberration coefficients that is based on Cartesian coordinates, and that would be applicable to systems with rectangular rather than rotational symmetry, would be a worthwhile endeavor, but will be left for the future.

The effects of aberrations on a spatially modulated IFTS depend partly on the nature of the source, which in turn will depend on the application. For stellar astronomy, no slit is required, but the sources are natural point sources. For remote sensing, a slit is required to obtain the second spatial dimension, so the source may be thought of as a line source. Finally, for some applications (perhaps in a limb-viewing instrument for atmospheric science) the source is extended, but spatial resolution is required only in the vertical direction. In this case no slit is required, and the source is extended in both dimensions. Some effects will occur for all three classes of source, while others are significant only for an extended source.

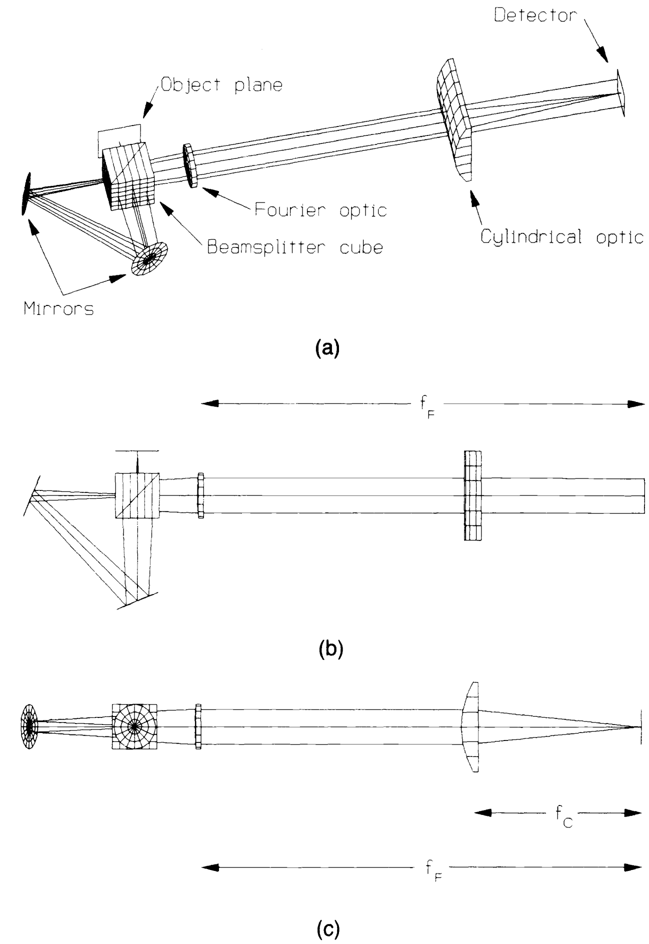


**Fig. 1** Layout drawing of a spatially modulated IFTS: (a) perspective view, (b) plan view, and (c) side view. The focal lengths of the Fourier optic and cylindrical optics are $f_F$ and $f_C$. For clarity, rays are shown only for the reflected path.

## 2 Effects That Occur with All Classes of Sources

If we consider a point source in the object plane, the interferometer splits it into two virtual point sources that are mutually coherent. As shown in Fig. 3, the Fourier optic collects the rays from each of the two sources and collimates them, producing a pair of flat wavefronts that interfere and thus produce a fringe pattern on the detector. For a monochromatic source of wavelength $\lambda$, the spatial frequency $\nu$ of this fringe pattern is given by Eq. (1), which can also be expressed in terms of the shear angle $\theta$:

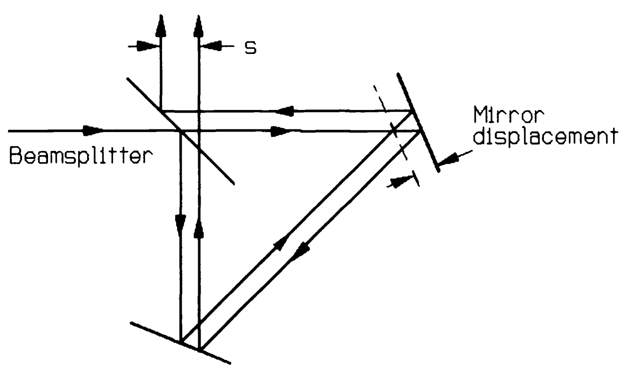


**Fig. 2** Raytrace showing source doubling in a Sagnac interferometer. The resulting separation between the virtual sources is *s*.

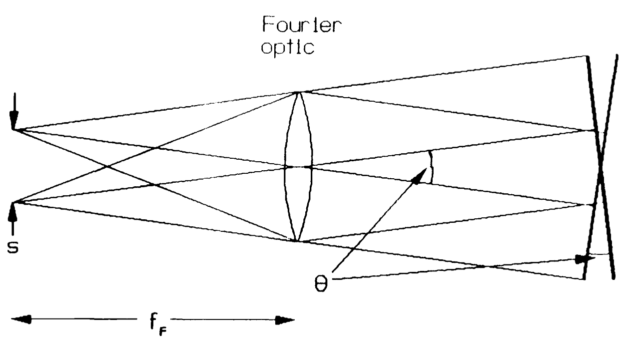


**Fig. 3** Raytrace showing the function of the Fourier optic to produce (ideally) flat wavefronts, with a shear angle θ.

$$\nu=\frac{\theta}{\lambda}\ , \tag{2}$$

where θ is as defined in Fig. 3. The effect of aberrations in the Fourier optic is to degrade the collimation, thus producing a range of shear angles across the aperture. Thus a monochromatic source will actually produce a fringe pattern with a spread of spatial frequencies $\Delta\nu$, and the Fourier transform of this fringe pattern will indicate a spread of wavelengths $\Delta\lambda$. The ultimate result is a loss of spectral resolution, such that the aberration-limited resolving power $R_a$ is given by

$$R_a=\frac{\theta}{\Delta\theta}\ , \tag{3}$$

where $R_a$ is defined as $\lambda/\Delta\lambda$, θ is defined as in Fig. 3, and $\Delta\theta$ is the angular spread caused by the aberrations of the Fourier optic. Note that although $R_a$ is not explicitly a function of wavelength, $\Delta\theta$ may vary with wavelength if the Fourier optic is a lens rather than a mirror.

There may be many different aberrations that contribute to this total $\Delta\theta$. They may vary with field angle, position in the aperture, wavelength, or any combination of these. It may be possible to calibrate the system to correct for those aberrations that vary with field or wavelength but are constant across the aperture. For example, it should be possible to correct for distortion and transverse chromatic aberration (lateral color), but not for spherical aberration or coma.

A straightforward method of predicting $\Delta\theta$ is to use an optical design program that allows multiple configurations and a customized merit function. This merit function computes the *shear angle* θ, which is the angle in the plane of the interferometer between a pair of rays, one of which is reflected at the beamsplitter (one *configuration*) and the other of which is the same ray transmitted at the beamsplitter. This shear angle is evaluated for several pairs of rays across the aperture, and the quadratic sum of the differences between these shear angles and the shear angle for the chief ray (the *nominal shear angle*) constitutes the merit function. The value of the merit function is then a prediction of the rms $\Delta\theta$ at that wavelength and field angle. The merit function could, of course, be constructed to evaluate this for several field angles and/or wavelengths.

In addition to the aberrations, the detector will also limit the spectral range and resolution of the system. As in any instrument, the spectral responsivity of the detector will limit the spectral range; but with a Fourier transform instrument, the number of pixels will also affect both the spectral range and the spectral resolution. If the interference pattern imaged by the detector were infinite in extent, then the spectral resolution in the Fourier transform of this pattern would be unlimited; but since the detector is, in fact, of finite extent, we are only able to sample a portion of the interference pattern. The resulting spectral resolution (in terms of wave numbers) is given by[5]

$$\Delta\sigma=\sigma_c\frac{1}{0.8N}\ , \tag{4}$$

where $\Delta\sigma$ is the detector-limited spectral resolution in wave numbers, $\sigma_c$ is the short-wavelength cutoff in wave numbers, and $N$ is the *effective* number of pixels across the detector in the plane of the interferometer (the number actually illuminated by the interference pattern). The factor of 0.8 is used because a small portion of the interferogram should also be measured on both sides of the zero-path-difference point in order to preserve phase information. This equation is given in terms of wave numbers (rather than wavelength resolution or resolving power) because $\Delta\sigma$ does not vary with wavelengths. If we convert Eq. (4) into wavelength terms, we see that the detector-limited resolving power $R_d$ does vary with wavelength:

$$R_d\simeq\frac{\lambda_c}{\lambda}0.8N\ , \tag{5}$$

where $\lambda_c=1/\sigma_c$ and the approximation holds while $\Delta\sigma$ is small compared to σ (or, equivalently, $\Delta\lambda$ is small compared to λ).

The shear angle θ is chosen to match the maximum spatial frequency that the detector can resolve to the spatial frequency corresponding to the desired short wavelength cutoff $\lambda_c$. If the pixel width is $x$, then the cutoff spatial frequency $\nu_c$ for the detector will be approximately given by

$$\nu_c=\frac{1}{2x}\ , \tag{6}$$

therefore, we set the shear angle to

$$\theta=\nu_c\lambda_c=\frac{\lambda_c}{2x}\ . \tag{7}$$

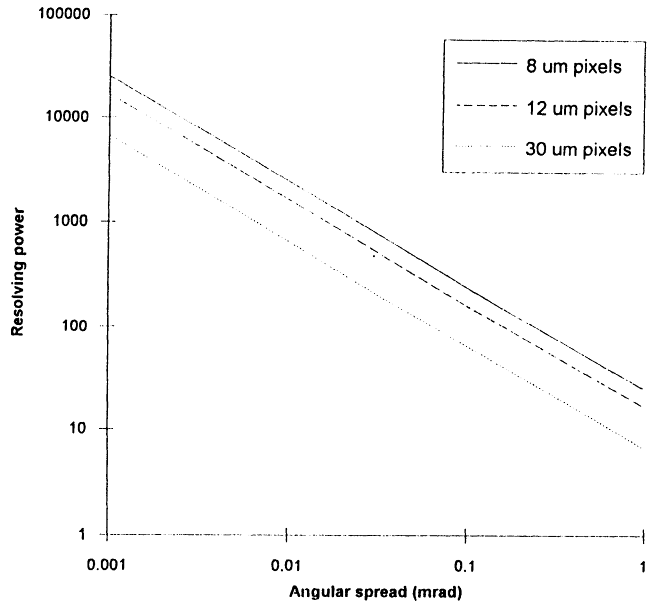


**Fig. 4** Predicted aberration-limited resolving power $R_a$ as a function of the angular spread $\Delta\theta$ due to aberrations, for three pixel widths $x=8$, 12, and 30 $\mu$m. The shear angle $\theta$ has been set for a cutoff wavelength of 400 nm.

As an example, consider an instrument with a cutoff wavelength of $\lambda_c=400$ nm. Given this cutoff wavelength and the pixel width $x$, the desired shear angle $\theta$ can be calculated using Eq. (7). The aberration-limited resolving power $R_a$ as a function of the angular spread $\Delta\theta$ can then be predicted by Eq. (3). This predicted aberration-limited resolving power is shown in Fig. 4 for three common CCD pixel widths. Note, however, that the resolving power could be limited either by this wavelength spread (caused by aberrations) or by the number of detector elements [according to Eq. (5)]. If the detector in this example had 1024 elements in the spectral direction, the detector-limited resolving power at the cutoff wavelength would be approximately 800. Thus, if the pixel width is 12 $\mu$m, then the spectral resolution will be limited by the number of detector elements $N$, rather than by the aberrations, if the $\Delta\theta$ due to aberrations can be kept below 0.05 mrad.

## 3 Effects That Occur Only with an Extended Source

Up to this point, we have considered only a point source or vertical line source, but if we have a source that is extended in the horizontal direction, then there are additional factors to consider. In the Sagnac interferometer, as in most interferometers, the path *difference* between a pair of rays (the reflected ray and the transmitted ray) is a function of the angle, but not the position, of the original ray as it enters the interferometer. This property, along with the Fourier optic, is what allows us to do without the slit required in a dispersive instrument. Since the detector is placed in the back focal plane of the Fourier optic, all the rays that pass through the interferometer at the same angle should be collected at the same point on the detector, as shown in Fig. 5. Thus, all of the rays that arrive at a particular point on the detector will have the same path difference and the same degree of interference. Any aberrations of the Fourier optic will result in rays from a *range* of angles being collected at the same point on the detector. This range of angles implies a range of degrees of interference, and ultimately results in a loss of modulation in the fringe pattern.

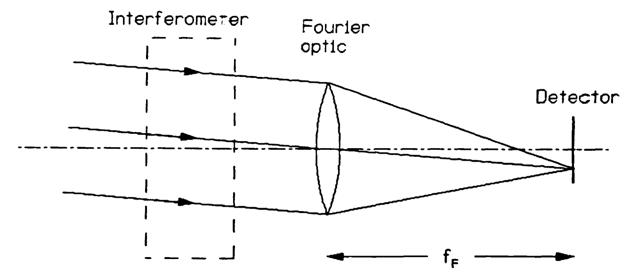


**Fig. 5** Raytrace showing the function of the Fourier optic to collect parallel rays at the same point on the detector.

When a Fourier transformation is performed on the fringe pattern, the strength of each component in the resulting spectrum is a function of the modulation of the corresponding spatial frequency in the fringe pattern. Thus, a loss in modulation at a particular spatial frequency causes a loss in responsivity at the wavelength corresponding to that spatial frequency. The spectral responsivity of the instruments is then a function of the modulation transfer function (MTF) of the optics, as well as the spectral transmittance and the spectral responsivity of the detector. Depending on the performance of the optics, this effect can cause virtually complete loss of modulation at the shorter wavelengths. Thus the effective short-wavelength cutoff may be determined by the optics rather than by the detector. Obviously, the optics should be designed to preserve some useful modulation at the spatial frequency corresponding to the desired short-wavelength cutoff.

In order to quanitify this effect we must examine the MTF (in the horizontal direction) of the combination of the Fourier and cylindrical optics. In this analysis the object must be placed at infinity, since we are interested in tracing rays that all passed through the interferometer at the same angle. Note that this implies that aberrations of the fore-optics do not need to be considered here; only aberrations introduced after the interferometer will contribute to this effect. The spatial frequencies for which we wish to maximize the modulation depend on the cutoff frequency of the detector, as discussed in Sec. 2. In order to achieve the highest modulation, we want to design the Fourier optic for infinite conjugate ratio, oriented for a collimated input.

Note, however, that maximization of the spectral resolution (as discussed in Sec. 2) requires the opposite orientation (collimated *output*). Thus, when we have an extended source, there must be a tradeoff between spectral resolution and modulation. If the Fourier optic is designed for infinite conjugate ratio, then one orientation will favor spectral resolution and the other will favor modulation. For a compromise between the two requirements, the Fourier optic should be designed for some finite conjugate ratio. Thus the designer should create several designs, each optimized for a different conjugate ratio. This will lead to a table of the expected spectral resolution and modulation for each design from which the preferred design can be selected.

It should be pointed out that this effect is not the only factor that will degrade the modulation. While not strictly an aberration, the transmittance/reflectance ratio of the beamsplitter also has a significant effect on the modulation of the interference pattern. The modulation (or visibility) $V$ of interference fringes in any two-beam interferometer is related to the beam amplitudes $E_1$ and $E_2$ by the following relation[7]:

$$V=\frac{2E_1E_2}{E_1^2+E_2^2} . \tag{8}$$

Thus, maximum modulation occurs when the two beams have equal amplitudes. In a Michelson interferometer, one beam is reflected and then transmitted, while the other is transmitted and then reflected by the beamsplitter, so the effects of an unequal split between reflectance and transmittance tend to cancel out. In a Sagnac interferometer, however, one beam is reflected twice while the other is transmitted twice, resulting in a modulation given by

$$V=\frac{2RT}{R^2+T^2} , \tag{9}$$

where $R$ and $T$ are the reflectance and transmittance of the beamsplitter. The resultant modulation is the product of this factor, the MTF of the optics (as discussed earlier in this section), and other effects such as stray light and detector bias (e.g., dark current).

## 4 Spatial Resolution and the Cylindrical Optic

Aberrations will also degrade the spatial resolution of the instrument, of course; and here the performance of the cylindrical optic and the fore-optics is important in addition to that of the Fourier optic. Since the effects of aberrations on spatial resolution are well known[6,8], they need not be discussed in detail here. It should be noted, however, that maximization of the spatial resolution favors designing the Fourier optic for collimated *output*. Designing for this conjugate ratio will also maximize the spectral resolution, but will have the opposite effect on the modulation (if the source is extended), as discussed in Sec. 3. This consideration adds a new element to the tradeoff between spectral resolution and modulation that must be considered when the source is extended. Both spectral and spatial resolution favor design for collimated output, whereas modulation favors design for collimated input.

The cylindrical optic may also have some effect on the spectral resolution and modulation (in addition to the Fourier optic), depending on the focal ratio and field of view. While there is not much that can be done to the design of the cylindrical optic itself in order to minimize these effects, it should be included with the Fourier optic when analyzing these effects.

## 5 The HYPO Instrument

In order to illustrate the effects we have discussed, we use the HYPO (hyperspectral plume observer) instrument as an example. This instrument was a spatially modulated IFTS designed for observations of launch-vehicle plumes from a ground-based telescope. It was the first, and least sophisticated, instrument we constructed, employing a 250-mm-focal-length singlet lens as the Fourier optic, and a singlet cylindrical lens as the cylindrical element. A calibration of this instrument was performed using a hydrogen emission lamp with a strong line at 656.3 nm. The raytrace analysis predicted a $\Delta\theta=0.13$ mrad at the 656.3-nm wavelength. The adjustable mirror was set for a shear angle $\theta=5.3$ mrad, so Eq. (3) predicts a resolving power $R_a=41$, which gives a wavelength resolution $\Delta\lambda=16$ nm at this wavelength. Analysis of the calibration results show an actual $\Delta\lambda$ for this line of about 16 nm. These results are summarized in Table 1.

**Table 1** Specifications and predicted aberration effects for the HYPO instrument. The values quoted here are for the center of the field of view.

| | |
|---|---|
| Effective detector elements N: | 493 |
| Detector-limited resolving power $R_d$ (at 656.3 nm): | 390 |
| Detector-limited spectral resolution (at 656.3 nm): | 1.7 nm |
| Desired cutoff wavelength $\lambda_c$: | 120 nm |
| Pixel width $x$: | 12 μm |
| Shear angle θ: | 5.3 mrad |
| Predicted angular spread Δθ (at 656.3 nm): | 0.13 mrad |
| Predicted aberration-limited resolving power $R_a$: | 41 |
| Predicted aberration-limited spectral resolution Δλ (at 656.3 nm): | 16 nm |
| Measured spectral resolution (at 656.3 nm): | 16 nm |

## 6 Conclusions

The effects of aberrations discussed here illustrate the importance of controlling the aberrations in a spatially modulated IFTS, particularly for applications that require good spatial or spectral resolution. The first step in designing such a system is to understand the effects that these aberrations will have on the performance of the instrument. This allows the designer to translate from the system specifications to a tolerance budget that explicitly includes the effects of aberrations in the optical elements.

The resolving power of an unaberrated system is determined by the number of pixels across the plane of the interferometer as given in Eq. (5). The shear angle θ should be set by the pixel width and the desired short wavelength cutoff, as shown in Eq. (7). The aberration-limited resolving power can then be calculated from Eq. (3); or conversely, the allowable spread in the shear angle Δθ can be calculated from the required resolving power. A graph such as Fig. 4 may be useful at this point in the design. The goal of this step will typically be to reach the detector-limited resolving power given by Eq. (5).

If the source is extended in the plane of the interferometer, then the resulting loss of modulation can be calculated from the horizontal MTF of the optics for a collimated input. In this case, the optics must be designed to preserve a useful degree of modulation at spatial frequencies up to $\nu_c$ (the cutoff spatial frequency for the detector). This requirement will drive the design of the Fourier optic to the opposite conjugate ratio from that required to maximize the spectral and spatial resolutions. Several iterations may be required in this design process in order to design a Fourier optic that satisfies both the resolution and the modulation requirements.

## Acknowledgments

We would like to thank Eirik Holbert for providing calibration data, and Joel Blatt for his helpful comments on this paper. This research was supported in part by DARPA and ONR through contract 9212 with the University of Hawaii.

## References

1. T. Okamoto, S. Kawata, and S. Minami, "Fourier transform spectrometer with a self-scanning photodiode array," *Appl. Opt.* **23**(2), 269–273 (1984).
2. T. H. Barnes, "Photodiode array Fourier transform spectrometer with improved dynamic range," *Appl. Opt.* **24**(22), 3702–3706 (1985).
3. J. V. Sweedler and M. B. Denton, "Spatially encoded Fourier transform spectroscopy in the ultraviolet to near-infrared," *Appl. Spectrosc.* **43**(8), 1378–1384 (1989).
4. M. L. Junttila, "Stationary Fourier-transform spectrometer," *Appl. Opt.* **31**(21), 4106–4112 (1992).
5. J. B. Rafert, P. G. Lucey, and H. Newby, "A spatially modulated imaging Fourier transform spectrometer for astronomical and booster plume observations," in *Proc. ESO Conf. on Progress in Telescope and Instrumentation Technologies*, Garching, Germany, European Southern Observatory (1992).
6. W. J. Smith, *Modern Lens Design*, McGraw-Hill, New York (1992).
7. E. Hecht and A. Zajac, *Optics*, p. 493, Addison-Wesley, Reading, MA (1974).
8. F. L. Pedrotti and L. S. Pedrotti, *Introduction to Optics*, p. 92, Prentice-Hall, Englewood Cliffs, NJ (1987).

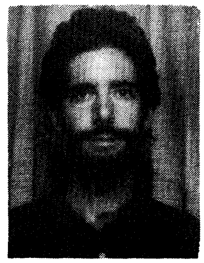

**R. Glenn Sellar** received his BEng in engineering physics from McMaster University in 1986 and his MS in space science from the Florida Institute of Technology in 1993. He has worked as an optical engineer for five years, in the space industry and in academia. His work has been concentrated on imaging spectrometers, including the WINDII instrument on the Upper Atmosphere Research Satellite. He is currently designing and building optical instrumentation as a research engineer at the Florida Institute of Technology.

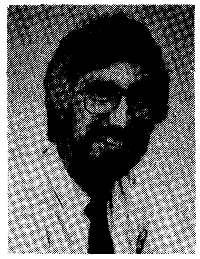

**J. Bruce Rafert** received his PhD in astronomy from the University of Florida in 1979, and is currently a professor of physics and space sciences at the Florida Institute of Technology. His research interests include the observational astrophysics of close binary star systems, the use of automatic telescopes, and space object identification of satellites and booster exhaust plumes using imaging Fourier transform spectrometers. He also serves as the director of Florida Tech's Center for Space Science Research and the chief scientist at the Phillips Laboratory Malabar Test Facility.